

Kinetics and Mechanisms of Oxygen Transfer in the Reaction of *p*-Cyano-*N,N*-dimethylaniline *N*-Oxide with Metalloporphyrin Salts. 3.¹ Catalysis by [*meso*-Tetrakis(2,6-dichlorophenyl)porphinato]iron(III) Chloride

C. Michael Dicken, T. C. Woon, and Thomas C. Bruice*

Contribution from the Department of Chemistry, University of California at Santa Barbara, Santa Barbara, California 93106. Received June 27, 1985

Abstract: Decomposition of *p*-cyano-*N,N*-dimethylaniline *N*-oxide (NO) catalyzed by [*meso*-tetrakis(2,6-dichlorophenyl)porphinato]iron(III) chloride ($(\text{Cl}_2\text{TPP})\text{Fe}^{\text{III}}\text{Cl}$) yields as products *p*-cyano-*N,N*-dimethylaniline (DA), *p*-cyano-*N*-methylaniline (MA), and formaldehyde (CH_2O ; solvent, 25 °C, N_2 atmosphere). Intermediate in the reaction are mono and bis NO complexes ($(\text{Cl}_2\text{TPP}(\text{Cl})\text{Fe}^{\text{III}}\text{NO})$ and $(\text{Cl}_2\text{TPP}(\text{NO})\text{Fe}^{\text{III}}\text{NO})$, respectively). Oxygen transfer from the complexed NO species to the iron porphyrin is rate-limiting and provides the higher valent iron(IV) salts ($(\text{Cl}_2\text{TPP}(\text{Cl})\text{Fe}^{\text{IV}}\text{O})^+$ and $(\text{Cl}_2\text{TPP}(\text{NO})\text{Fe}^{\text{IV}}\text{O})^+$) and DA. The observed kinetics for reactions involving 10–100 turnovers of catalyst dictate that the catalyst is saturated in the formation of $(\text{Cl}_2\text{TPP}(\text{Cl})\text{Fe}^{\text{III}}\text{NO})$ and that formation of $(\text{Cl}_2\text{TPP}(\text{NO})\text{Fe}^{\text{III}}\text{NO})$ is unfavorable. The two iron(IV)-oxo porphyrin π -cation radical species are converted back to the iron(III) porphyrin catalytic moieties by oxidation of $\text{DA} \rightarrow \text{MA} + \text{CH}_2\text{O}$ and oxidation of CH_2O . Addition of 2,4,6-tri-*tert*-butylphenol (TBPB), 2,3-dimethyl-2-butene (TME), and cyclohexene results in the formation of TBP \cdot and the respective epoxides, thus inhibiting the oxidation of DA and CH_2O . The kinetics of the overall reaction and formation of each product may be simulated by employing the reactions of Scheme II and eq 1–r, and from the simulations, the rates and equilibria, leading to the formation of the two iron(IV)-oxo porphyrin π -cation radical species may be determined as can minimal rate constants for the oxidations of DA, CH_2O , and TBPB and the epoxidation of TME and cyclohexene. The results obtained herein with the electron-deficient porphyrin, $(\text{Cl}_2\text{TPP})\text{Fe}^{\text{III}}\text{Cl}$, are discussed and compared to those obtained previously when employing $(\text{TPP})\text{Fe}^{\text{III}}\text{Cl}$ as the catalyst.

N,N-Dimethylaniline *N*-oxides transfer their oxygen atoms to iron(III) and manganese(III) porphyrins following their ligation to these entities.^{1,2} Heteroaromatic amine *N*-oxides, such as pyridine *N*-oxide, ligate to metalloporphyrins but do not enter into the oxygen-transfer reaction. These differences in oxygen-transfer

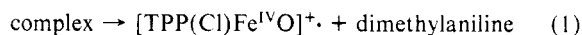
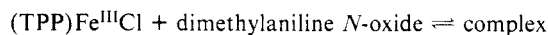
(1) (a) Shannon, P.; Bruice, T. C. *J. Am. Chem. Soc.* **1981**, *103*, 4500. (b) Nee, M. W.; Bruice, T. C. *J. Am. Chem. Soc.* **1982**, *104*, 6123. (c) Powell, M. F.; Pai, E. F.; Bruice, T. C. *J. Am. Chem. Soc.* **1984**, *106*, 3277. (d) Dicken, C. M.; Lu, F.-L.; Nee, M. W.; Bruice, T. C. *J. Am. Chem. Soc.* **1985**, *107*, 5776.

(2) On the basis of the data presented in this manuscript, in the studies listed in ref 1, and in the reaction of aniline *N*-oxides with cytochromes P-450_{LM2} and P-450_{CAM} (cf.: Heimbrook, D. C.; Murray, R. I.; Egeberg, H. D.; Sligar, S. G.; Nee, M. W.; Bruice, T. C. *J. Am. Chem. Soc.* **1984**, *106*, 1514), the mechanistic postulations of Burka, et al. (see: Burka, L. T.; Guengerich, F. P.; Willard, R. J.; Macdonald, T. L. *J. Am. Chem. Soc.* **1985**, *107*, 2549) may be disregarded. Burka and co-workers have stated "*N,N*-dimethylaniline *N*-oxides are not really able to oxidize ferric cytochrome P-450 or Mn^{III} or Cr^{III} (porphyrins) to +V hypervalent states"—"... direct two-electron oxidative cleavage of the $\text{Fe}-\text{O}-\text{N}$ complex (i.e., iron(III) porphyrin complex with *N*-oxide) to generate a formal $\text{Fe}^{\text{V}}=\text{O}$ species and an amine appears incompatible with ...". Concerning the cytochrome P-450 reaction, the results of Heimbrook et al. (loc. cit.) suffice to explain the experimental results of Burka et al. With regard to the transfer of *N*-oxide oxygen to manganese(III) tetraphenylporphyrin, this is shown to occur in the paper by Powell et al. (ref 1c). The transfer of oxygen from *p*-cyano-*N,N*-dimethylaniline *N*-oxide to chromium(III) tetraphenylporphyrin has been established to be a photocatalytic chain reaction (Yuan, L.-C.; Bruice, T. C. *J. Am. Chem. Soc.* **1985**, *107*, 512; Yuan, L.-C.; Calderwood, T. S.; Bruice, T. C. *Ibid.*, in press). In regard to the subject of the present manuscript, there is no doubt but that the oxygen from the *p*-cyano-*N,N*-dimethylaniline *N*-oxide (NO) is transferred to the iron(III) tetraphenylporphyrin ($(\text{TPP})\text{Fe}^{\text{III}}\text{Cl}$). Thus, from the experiments of Dicken et al. (ref 1d), it was shown that the first-order rate constant for product appearance in the reaction of NO with $(\text{TPP})\text{Fe}^{\text{III}}\text{Cl}$ to yield *p*-cyano-*N,N*-dimethylaniline (DA) and its oxidation products (see eq 2–5) exhibits a linear dependence on $[(\text{TPP})\text{Fe}^{\text{III}}\text{Cl}]$ and zero-order dependence on $[\text{NO}]$. In the presence of the 1e[−] acceptor trap, 2,4,6-tri-*tert*-butylphenol (TBPB), and the "oxene" acceptor trap, 2,3-dimethyl-2-butene (TME), the kinetics of the reaction are independent of $[\text{TBPB}]$ or $[\text{TME}]$. Most importantly, for both the one-electron trap, TBPB, and the "oxene" trap, TME, the products are DA (100%) and the radical TBP \cdot (100%) or the 2,3-dimethyl-2-butene epoxide (100%) and DA (100%). There can be only one explanation for these experimental results. Oxygen is transferred from the *N*-oxide to the iron(III)porphyrin in a rate-determining step to yield DA and $\cdot^+(\text{TPP})\text{Fe}^{\text{IV}}\text{O}$, and the latter species is trapped by 1e[−] transfer to yield TBP \cdot or oxygen transfer to yield the epoxide.

Table I. Effect of 2,4,6-Tri-*tert*-butylphenol Concentration on the Percentage Yields (Based upon the Initial Concentration of NO = 2.4×10^{-3} M) of 2,4,6-Tri-*tert*-butylphenoxyl Radical (TBP \cdot), DA, and MA. Concentration of $(\text{Cl}_2\text{TPP})\text{Fe}^{\text{III}}\text{Cl}$ Catalyst = 8.0×10^{-5} M

$[\text{TBPB}]_0$, M	% DA	% MA	% TBP \cdot
0.03	54	44	37
0.06	60	36	48
0.15	72	28	67
0.30	78	20	79

ability reflect the ease of reduction of aliphatic amine *N*-oxides and the difficulty in the reduction of heteroaromatic amine *N*-oxides.³ The direct products of the reaction of (*meso*-tetraphenylporphinato)iron(III) chloride and a dimethylaniline *N*-oxide are an *N,N*-dimethylaniline and an iron(IV)-oxo porphyrin π -cation radical (eq 1). An enzyme-bound iron(IV)-oxo porphyrin



π -cation radical species (compound I) is formed on reaction of peroxidases with hydrogen peroxide, alkyl hydroperoxides, or percarboxylic acids.⁴ Similar chemistry has been presumed in the "Peroxide Shunt" reactions of the cytochrome P-450 enzymes.⁵

p-Cyano-*N,N*-dimethylaniline *N*-oxide (NO) has proven to be a particularly useful reagent for the study of both the dynamics of formation and reactions of higher valent iron-oxo and manganese-oxo porphyrin species.¹ A detailed investigation of the reaction of NO with (*meso*-tetraphenylporphinato)iron(III) chloride has been reported.^{1d} Under the pseudo-first-order conditions of $[\text{NO}] \gg [(\text{TPP})\text{Fe}^{\text{III}}\text{Cl}]$, transfer of oxygen (eq 2) is rate-determining. As shown in eq 3, 4, and 5, oxygen transfer

(3) Katritzky, A. R.; Lagowski, J. M. "Chemistry of the Heterocyclic *N*-Oxides"; Academic Press: New York, 1971; Vol. 19, Chapter 3.

(4) (a) Morrison, M.; Schonbaum, G. R. *Ann. Rev. Biochem.* **1976**, *45*, 861. (b) Dunford, H. B.; Stillman, J. S. *Coord. Chem. Rev.* **1976**, *19*, 187.

(5) Groves, J. T. *Adv. Inorg. Biochem.* **1979**, 119.

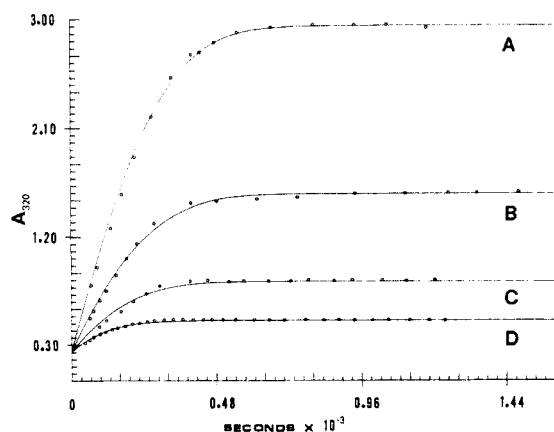


Figure 1. Experimental points for the appearance of DA and MA with time, as monitored at 320 nm which accompanies the reaction of $(\text{Cl}_8\text{TPP})\text{Fe}^{\text{III}}\text{Cl}$ at $8.0 \times 10^{-5} \text{ M}$ with varying concentrations of NO (the concentrations of NO employed are (A) $8.0 \times 10^{-3} \text{ M}$, (B) $4.0 \times 10^{-3} \text{ M}$, (C) $1.6 \times 10^{-3} \text{ M}$, (D) $8.0 \times 10^{-4} \text{ M}$). The lines which correlate the experimental points have been computer-generated by simulation using the reactions of Scheme II and the rate constants of Table IV.

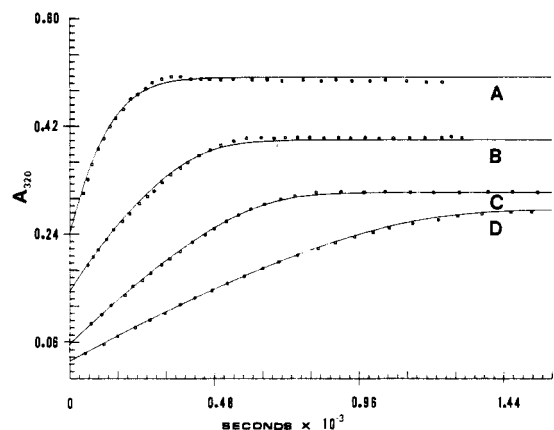


Figure 2. Experimental points for the change in absorbance at 320 nm with time which accompanies the reaction of NO ($7.7 \times 10^{-4} \text{ M}$) with $(\text{Cl}_8\text{TPP})\text{Fe}^{\text{III}}\text{Cl}$ at varying concentrations (the concentrations of $(\text{Cl}_8\text{TPP})\text{Fe}^{\text{III}}\text{Cl}$ employed are (A) $7.7 \times 10^{-5} \text{ M}$, (B) $3.8 \times 10^{-5} \text{ M}$, (C) $1.5 \times 10^{-5} \text{ M}$, (D) $7.7 \times 10^{-6} \text{ M}$). The lines which correlate the experimental points have been computer-generated by simulation using Scheme II and the rate constants of Table IV with the exception of k_5 which varies in the following manner: A, $3.0 \times 10^{-2} \text{ s}^{-1}$; B, $4.5 \times 10^{-2} \text{ s}^{-1}$; C, $9.0 \times 10^{-2} \text{ s}^{-1}$; D, $10.0 \times 10^{-2} \text{ s}^{-1}$.

remains intact for all the reactions described herein as evidenced from its visible spectrum at t_∞ .

Under the conditions of $[\text{NO}]_i \gg [(\text{Cl}_8\text{TPP})\text{Fe}^{\text{III}}\text{Cl}]_i$ and at constant iron(III) porphyrin concentration, the overall rate of the reaction when monitored at 320 nm does not vary appreciably with a change in $[\text{NO}]_i$. The initial rate constants show an increase with an increase in $[\text{NO}]_i$ (Figure 1). Changes in the iron(III) porphyrin concentration result in an appreciable change in the overall rates of product formation (Figure 2). In Figures 1 and 2, the points are experimental and the lines are computer-generated as best fits of the preferred reaction sequence (Discussion section).

Oxidation of 2,4,6-tri-*tert*-butylphenol (TBPH) in the presence of NO catalyzed by $(\text{Cl}_8\text{TPP})\text{Fe}^{\text{III}}\text{Cl}$ was followed at the λ_{max} of the phenoxyl radical (TBP \cdot) at 630 nm ($\epsilon_{630} 4.0 \times 10^2 \text{ M}^{-1} \text{ cm}^{-1}$), and the percentage yields of products were determined at the completion of the reaction (Table I). Examination of Table I shows that an increase in $[\text{TBPH}]_i$ is accompanied by an increase in the yield of TBP \cdot and DA and a decrease in the yield of MA. These results find ready explanation in the sense of eq 9 which shows a means for competition of TBPH with DA for the higher valent iron-oxo porphyrin π -cation species. At the highest con-

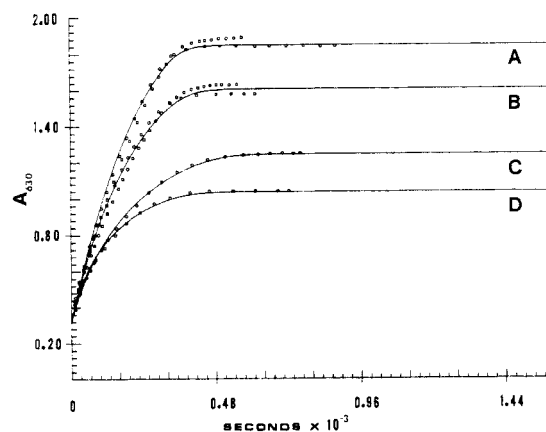
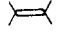
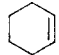
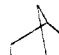
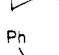



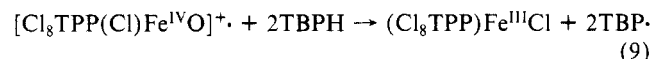
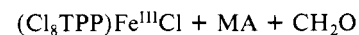
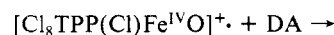
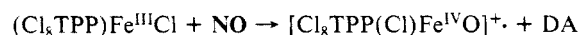
Figure 3. Spectral time course for the oxidation of TBPH monitored at $\lambda_{\text{max}} = 630 \text{ nm}$ for the radical TBP \cdot . In these experiments, the $[\text{NO}]_i$ and the $[(\text{Cl}_8\text{TPP})\text{Fe}^{\text{III}}\text{Cl}]_i$ have been maintained at 2.4×10^{-3} and $8.0 \times 10^{-5} \text{ M}$, respectively. The concentrations of TBPH are as follows: A, 0.30 M; B, 0.15 M; C, 0.06 M; D, 0.03 M. The experimental points have been fitted with computer-generated lines by employing the reactions of Scheme II and eq n-q with associated rate constants as discussed in the manuscript.

Table II. Oxidation of Alkenes by NO Catalyzed by $(\text{Cl}_8\text{TPP})\text{Fe}^{\text{III}}\text{Cl}$ and $(\text{TPP})\text{Fe}^{\text{III}}\text{Cl}$

substrate	% yield of epoxide ^a	
	$(\text{Cl}_8\text{TPP})\text{Fe}^{\text{III}}\text{Cl}$	$(\text{TPP})\text{Fe}^{\text{III}}\text{Cl}$ catalyzed
	25	90
	34	45
	0	36
	0	29
	0	17

^a GC yields are based on $[\text{NO}]_i$.

centration employed, the TBPH has yet to trap all the higher valent iron-oxo porphyrin π -cation species (Table I).



In Figure 3 there is shown the change in A_{630} with time that accompanies the reactions of Table I. Examination of Figure 3 shows that the presence of TBPH has no effect on the rate of the overall reaction. The points in Figure 3 are experimental and the correlation lines computer-generated through the use of a competent reaction sequence (see Discussion section).

Reaction of NO ($2.7 \times 10^{-3} \text{ M}$) with $(\text{Cl}_8\text{TPP})\text{Fe}^{\text{III}}\text{Cl}$ ($8.0 \times 10^{-5} \text{ M}$) in the Presence of a Number of Alkenes (1.0 M). The percentage yields of epoxides (determined by capillary GC (see Experimental Section)) are given in Table II and compared to those obtained with $(\text{TPP})\text{Fe}^{\text{III}}\text{Cl}$ as the catalyst.^{1d} From Table II, $(\text{TPP})\text{Fe}^{\text{III}}\text{Cl}$ is seen to be the better catalyst. In fact, with $(\text{Cl}_8\text{TPP})\text{Fe}^{\text{III}}\text{Cl}$, only cyclohexene and 2,3-dimethyl-2-butene (TME) show any ability to compete with the demethylation reaction of DA to yield MA. The percentage yields of TME-epoxide, DA, and MA obtained when TME is employed as a substrate are provided in Table III. The addition of TME as a substrate has little effect on the kinetics of the turnover reaction of NO with

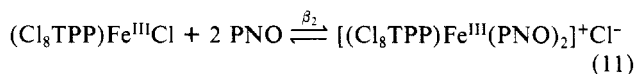
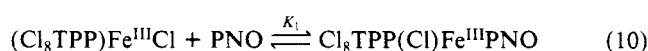
(8) Nash, T. *Biochem. J.* **1953**, *55*, 416.

Table III. Effect of 2,3-Dimethyl-2-butene (TME) on the Product Yields in the (Cl₈TPP)Fe^{III}Cl (8.0 × 10⁻⁵ M) Catalyzed Decomposition of NO (2.7 × 10⁻³ M)

[TME] _i , M	% DA	% MA	% TME-epoxide
	36	60	
0.01	36	58	1
0.10	44	54	6
1.00	51	46	24

the iron(III) porphyrin except at its highest concentrations where the rate becomes slightly slower (Figure 4).

Equilibrium Constants for the ligation of picoline *N*-oxide (PNO) with (Cl₈TPP)Fe^{III}Cl were approximated by the visible spectral techniques of Walker and co-workers.⁹ Picoline *N*-oxide has been employed since it is unable to transfer its oxygen to the iron(III) porphyrin. The equilibrium binding of PNO was followed at 510 nm where an α,β absorbance band of the iron(III) porphyrin disappears upon its complexation. The approximated equilibrium constants of eq 10 and 11 were calculated to be 70 M⁻¹ and 830 M⁻², respectively. Though useful in the determi-

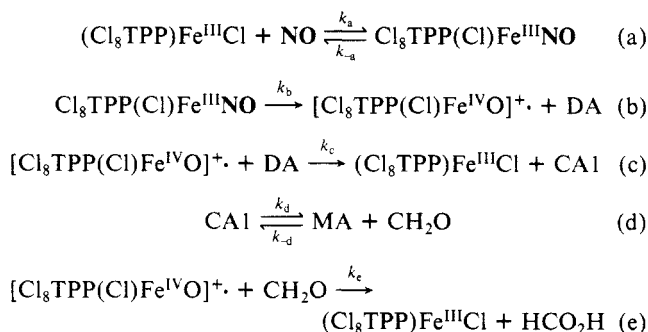


nation of the propensity of metalloporphyrins to complex one and two axial ligands ($\beta_2/K_1 = 10$), the implicit assumption is made in Walker's derivation that the extinction coefficient for the 1:1 complex is similar to the extinction coefficient for the 2:1 complex. This may or may not be so. The inability to determine the extinction coefficient of the 1:1 complex warrants the use of this method.

Discussion

The reaction of *p*-cyano-*N,N*-dimethylaniline *N*-oxide (NO) with [*meso*-tetrakis(2,6-dichlorophenyl)porphinato]iron(III) chloride ((Cl₈TPP)Fe^{III}Cl) (25 °C, CH₂Cl₂ solvent, anaerobic) provides as products *p*-cyano-*N,N*-dimethylaniline (DA), *p*-cyano-*N*-methylaniline (MA), and formaldehyde. The iron(III) porphyrin is not consumed. The percentage yields of the products and the dynamics for MA and DA formation have been determined at various concentrations of both NO and iron(III) porphyrin salt. Formation of DA and MA with time was followed spectrophotometrically at 320 nm where absorbance of the iron(III) porphyrin salt is minimal. Computer fitting of the experimentally determined changes in A₃₂₀ with time has been carried out by using various assumed reaction schemes and the extinction coefficients of DA and MA at 320 nm. The most simplistic reaction sequence is provided in Scheme I (where CA1 is the carbinolamine of MA with CH₂O). In Scheme I, axial

Scheme I

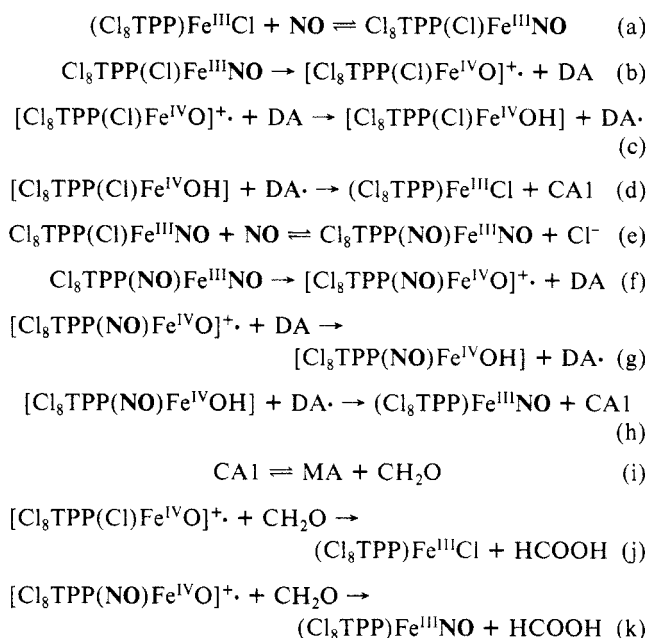


complexation of NO by iron(III) porphyrin (eq a) is followed by the rate-determining oxygen transfer (eq b) to generate an iron(IV)-oxo porphyrin π-cation radical and DA. There then

follows the oxidation of DA to CA1, dissociation of CA1 to MA and formaldehyde, and oxidation of formaldehyde.

Unlike the reaction of (TPP)Fe^{III}Cl with NO, we were not able to completely trap the iron(IV)-oxo octachloroporphyrin π-cation radical (eq b) and thereby determine independently the rate constant for the commitment step of oxygen transfer from NO to iron(III) octachloroporphyrin. Each of the plots of Δ₃₂₀ vs. time with change in the initial concentration of NO ([NO]_i) (Figure 1) could be fit by using the reaction sequences of Scheme I if iteration of the rate constants for each of the kinetic plots were carried out separately. In each instance, it was necessary that the equilibrium constant k_a/k_{-a} be such that the iron(III) porphyrin catalyst be saturated in NO through most of the time course for the reactions. Since the apparent rate constants, k_a/k_{-a} and k_b , were [NO]_i-dependent, in going from plot to plot, Scheme I does not provide a unifying rate law. A plot of the k_b values vs. [NO]_i was found to be linear. Thus, the reaction is at least partially second-order (slope of plot) in [NO]_i. With this in mind, the rate-determining steps may be taken to involve decomposition of both the mono and bis complexes Cl₈TPP(Cl)Fe^{III}NO and Cl₈TPP(NO)Fe^{III}NO. From our experience in generating the simulations with Scheme I, formation of Cl₈TPP(Cl)Fe^{III}NO must be exergonic at the concentrations of NO employed. Saturation of the catalyst by formation of the mono NO ligated complex and the role of a bis complex in the product formation have been incorporated into Scheme II. (In the sequence of reactions in Scheme II, each step pertains to the rate-controlling process and not to convey, necessarily, the mechanism of the reaction. Thus, reactions c and g likely occur by rate-controlling electron abstraction followed by proton transfer from carbon.)

Scheme II



The following assumptions and restrictions were employed in arriving at the rate constants for the reactions of Scheme II: (i) The rate constants for the 1e⁻ oxidation of DA by the two iron(IV)-oxo porphyrin π-cation radical species have been assumed to be equal ($k_c = k_g$); (ii) The rate constants for the oxidation of CH₂O by the two iron(IV)-oxo porphyrin π-cation radical species are taken as equal ($k_j = k_k$); (iii) The equilibrium constant for dissociation of carbinolamine to MA and CH₂O is taken as that determined in a previous study ($k_i/k_{-i} = 10/130$ to $1 \times 10^8/1.3 \times 10^9$ M; any value in this range is suitable); (iv) The rate constants for 1e⁻ oxidation of DA[•] by both iron(IV)-oxo porphyrin species are taken as diffusion-controlled as before ($k_d = k_h = 10^9$ M⁻¹ s⁻¹). Determination of unassigned rate constants was carried out by iteration. The value of k_a/k_{-a} must be large enough to provide sufficient "zero orderness" to the plots of ΔA₃₂₀ vs. time. This requires a value for k_a/k_{-a} that is approximately

(9) Walker, F. A.; Lo, M.-W.; Ree, M. T. *J. Am. Chem. Soc.* **1976**, *98*, 5552.

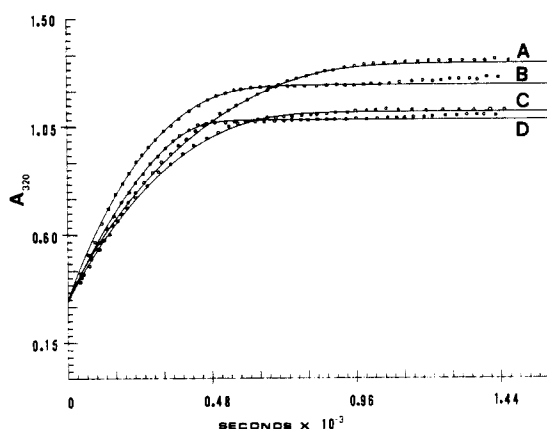


Figure 4. Experimental points for the change in absorbance at 320 nm with time due to the formation of DA and MA on reaction of NO (2.7×10^{-3} M) and $(\text{Cl}_8\text{TPP})\text{Fe}^{\text{III}}\text{Cl}$ (8.0×10^{-5} M) in the presence of TME where the concentration is (A) 1.00 M, (B) 0.10 M, (C) 0.01 M, and (D) not present during the reaction. The lines which correlate the experimental points have been computer-generated from Scheme II and eq 1 and m as discussed in the manuscript.

Table IV. Rate Constants Employed To Fit the Experimental Points of Figure 1 (Using Scheme II) which Shows the Dependence of Kinetics and Product Yields on $[\text{NO}]_i$ at $[(\text{Cl}_8\text{TPP})\text{Fe}^{\text{III}}\text{Cl}] = 8.0 \times 10^{-5}$ M

k_a/k_{-a}	$1.0 \times 10^5/10.0 \text{ M}^{-1}$
k_b	$4.0 \times 10^{-2} \text{ s}^{-1}$
$k_c = k_g$	$3.4 \times 10^5 \text{ M}^{-1} \text{ s}^{-1}$
$k_d = k_h$	$1.0 \times 10^9 \text{ M}^{-1} \text{ s}^{-1}$
k_e/k_{-e}	$1.5 \times 10^3/10.0$
k_f	0.47 s^{-1}
k_i/k_{-i}	$1.0 \times 10^3/1.3 \times 10^4 \text{ M}$
$k_j = k_k$	$4.4 \times 10^5 \text{ M}^{-1} \text{ s}^{-1}$

100 times greater than that found for the complexing of picoline *N*-oxide. Apparently, heteroaromatic *N*-oxides do not bind as well to iron(III) porphyrins as do dimethylaniline *N*-oxides. Other portions of the plots are shaped by the choice of the values of k_b , k_e/k_{-e} , and k_f . The correct percentage yields of DA, MA, and CH_2O are set by the correct choice of k_c/k_j . Successful curve fitting is dependent upon the setting of the values of $k_c = k_g$ and $k_j = k_k$ at some minimal set in order to obviate the prediction of a lag phase in the increase of A_{320} with time (since none is seen experimentally). Increasing the values of k_c , k_g , k_j , and k_k beyond their assigned minimal values has no influence upon the fitting of the experimental data. These constants pertain to the oxidations carried out by the iron(IV)-oxo porphyrin π -cation species. Since these reactions follow the rate-determining step (transfer of an oxygen from *N*-oxide to iron(III) porphyrin), their rate constants cannot be assigned an absolute value without discrete characteristics of the dynamics for the formation of products. The lack of an experimentally detectable lag phase in product formation allows the setting of their values at a minimum but no information is provided in the dynamics of product formation which allows the setting of maximum values.

The constants of Table IV have been employed with Scheme II to generate the lines which correctly correlate the experimental points of Figure 1 for the dependence upon $[\text{NO}]_i$ of DA and MA appearance with time. None of the constants of Table IV exhibit a dependency upon $[\text{NO}]_i$, and the experimental kinetic points are fit within the accuracy of the spectrophotometer to the completion of reaction (10–100 turnovers of iron porphyrin catalyst). Scheme II is, therefore, a competent expression of the reaction insofar that its use provides a correct correlation of the time course for DA and MA formation and yields of DA, MA, and CH_2O when $[\text{NO}]_i$ is varied at a particular concentration of $(\text{Cl}_8\text{TPP})\text{Fe}^{\text{III}}\text{Cl}$ (8×10^{-5} M). In Table IV, k_e/k_{-e} for the formation of the bis NO complex has been simulated as 100 times less than k_a/k_{-a} for the formation of the mono NO complex. It has been determined experimentally (Results section) that the

Table V. Effect of $[\text{NO}]_i$ on the Oxidation of DA and CH_2O by a Bis Complex vs. a Mono Complex (Initial Concentration of $(\text{Cl}_8\text{TPP})\text{Fe}^{\text{III}}\text{Cl} = 8.0 \times 10^{-5}$ M)

$[\text{NO}]_i$, M	$[(\text{Cl}_8\text{TPP}(\text{NO})\text{Fe}^{\text{IV}}\text{O})^+ \cdot]_{\text{max}}/[(\text{Cl}_8\text{TPP}(\text{Cl})\text{Fe}^{\text{IV}}\text{O})^+ \cdot]_{\text{max}}$
8.0×10^{-3}	23.14
4.0×10^{-3}	9.88
1.6×10^{-3}	3.46
8.0×10^{-4}	2.26

Table VI. Effect of $[(\text{Cl}_8\text{TPP})\text{Fe}^{\text{III}}\text{Cl}]_i$ on the Oxidation of DA and CH_2O by a Bis Complex vs. a Mono Complex (Initial Concentration of NO = 7.7×10^{-4} M)

$[(\text{Cl}_8\text{TPP})\text{Fe}^{\text{III}}\text{Cl}]_i$, M	$[(\text{Cl}_8\text{TPP}(\text{NO})\text{Fe}^{\text{IV}}\text{O})^+ \cdot]_{\text{max}}/[(\text{Cl}_8\text{TPP}(\text{Cl})\text{Fe}^{\text{IV}}\text{O})^+ \cdot]_{\text{max}}$
7.7×10^{-5}	1.93
3.8×10^{-5}	0.63
1.5×10^{-5}	0.31
7.7×10^{-6}	0.29

formation of the bis complex with picoline *N*-oxide (PNO) is 5 times less than that for the formation of the mono PNO complex. Thus, though complexing of NO as an axial ligand is greatly favored over the complexing of PNO to yield monocomplexes (loc. cit.), the equilibrium constants for complexing of the second NO or PNO moieties differ by less than an order of magnitude.

The influence upon the kinetics in changing the concentration of the $(\text{Cl}_8\text{TPP})\text{Fe}^{\text{III}}\text{Cl}$ catalyst at a constant initial concentration of NO (7.7×10^{-4} M) is shown in Figure 2. The experimental points of Figure 2 have been fit by computer-generated lines using the reaction sequence of Scheme II and, with the exception of k_b , the constants of Table IV. In order to fit the experimental points of Figure 2, it has been necessary to allow k_b a dependence upon iron(III) porphyrin concentrations:

$[(\text{Cl}_8\text{TPP})\text{Fe}^{\text{III}}\text{Cl}]_i$, M	k_b , s^{-1}
7.7×10^{-6}	10×10^{-2}
15×10^{-6}	9.0×10^{-2}
38×10^{-6}	4.5×10^{-2}
77×10^{-6}	3.0×10^{-2}

The increase in k_b of ~ 3 -fold on decrease of the iron(III) porphyrin concentration by 10-fold reflects a modest increase in rate and a greater "zero-order character" in the change of A_{320} with time on a decrease in catalyst concentration. This may reflect stabilization of the $\text{Cl}_8\text{TPP}(\text{Cl})\text{Fe}^{\text{III}}\text{NO}$ species or destabilization of the transition state for the oxygen-transfer step caused by self-association of the $\text{Cl}_8\text{TPP}(\text{Cl})\text{Fe}^{\text{III}}\text{NO}$ moiety.

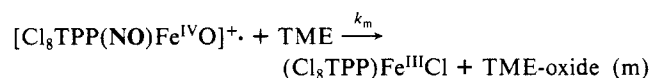
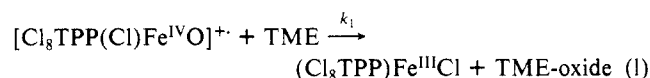
The importance of the mono and bis *N*-oxide complexes in the generation of iron(IV) porphyrin π -cation species as a function of $[\text{NO}]_i$ is seen in Table V. Increasing the $[\text{NO}]_i$ by 10-fold causes the ratio of $[(\text{Cl}_8\text{TPP}(\text{NO})\text{Fe}^{\text{IV}}\text{O})^+ \cdot]_{\text{max}}/[(\text{Cl}_8\text{TPP}(\text{Cl})\text{Fe}^{\text{IV}}\text{O})^+ \cdot]_{\text{max}}$ to increase by over 10-fold. The concentrations of NO considered in Table IV are those employed in the experiments of Figure 1. The maximum concentrations of Cl^- and NO-ligated iron(IV)-oxo porphyrin π -cation radicals generated during the reaction were determined by simulation from Scheme II employing the appropriate rate constants. The bis *N*-oxide complex is seen to play a major role in the overall rate of reaction at the higher turnovers of the catalyst. The importance of the reaction path through the bis complex also becomes more important on increasing $[(\text{Cl}_8\text{TPP})\text{Fe}^{\text{III}}\text{Cl}]_i$ (Table VI). However, the effect is not as great since a 10-fold change in the initial porphyrin concentration corresponds to a ~ 6 -fold change in the ratio of $[(\text{Cl}_8\text{TPP}(\text{NO})\text{Fe}^{\text{IV}}\text{O})^+ \cdot]_{\text{max}}/[(\text{Cl}_8\text{TPP}(\text{Cl})\text{Fe}^{\text{IV}}\text{O})^+ \cdot]_{\text{max}}$.

When 2,3-dimethyl-2-butene (TME) is included in the reaction mixture, the ratio of DA/MA products is increased, and epoxidation of the alkene occurs (Table III). This reflects the deflection of the iron(IV)-oxo porphyrin π -cation radical species from DA oxidation, yielding MA, to epoxidation of alkene. In all cases, the sum of $[\text{HCOOH}] + [\text{MA}] + [\text{TME-oxide}]$ products equals the oxidizing equivalents of NO employed. Figure 4 shows the increase in absorbance with time on reaction of NO ($=2.4 \times$

Table VII. Percentage Yields of Products Predicted by Computer Simulation for the Decomposition of NO ($=2.4 \times 10^{-3}$ M) Catalyzed by (Cl₈TPP)Fe^{III}Cl ($=8.0 \times 10^{-5}$ M) in the Presence of TME

% yields based on [NO] _i			
[TME] _i , M	DA	MA	TME-epoxide
0	40	60	0
0.01	40	59	1
0.10	42	58	6
1.0	54	46	28

10⁻³ M) with (Cl₈TPP)Fe^{III}Cl ($=8.0 \times 10^{-5}$ M) in the presence of varying concentrations of TME. For computer fitting of the experimental points of Figure 4, Scheme II was amended by the addition of eq l and m. In order to obtain the correct ratio of

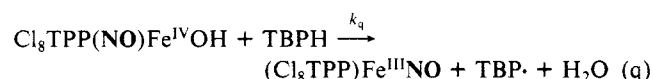
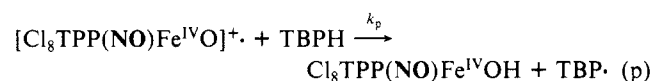
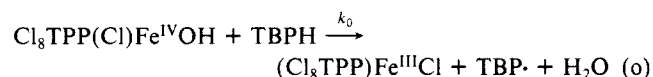
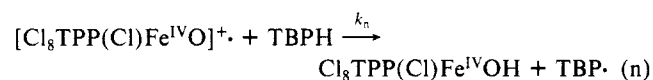


the products (TME-epoxide:DA:MA:CH₂O), k_l and k_m were set relative to k_c and k_f . Values of $k_l = k_m$ equal to $10^2 \text{ M}^{-1} \text{ s}^{-1}$ were found to serve this purpose. The iterative process established that best fits were obtained when k_b was allowed to change somewhat. The value of k_f required adjustment also but only at the highest concentration of TME:

[TME] _i , M	k_b , s ⁻¹	k_f , s ⁻¹
0	5.0×10^{-2}	0.47
0.10	2.5×10^{-2}	0.47
0.10	3.0×10^{-2}	0.47
1.0	2.0×10^{-2}	0.28

The values of k_b and k_f at [TME] = 1.0 M may presumably be attributed to a change in the nature of the CH₂Cl₂ solvent with such a high hydrocarbon content. Since $k_b = (3.5 \pm 1.0) \times 10^{-2} \text{ s}^{-1}$ and k_f shows no variation from 0.47 s⁻¹, Scheme II, with the rate constants of Table IV (plus eq l and m with $k_l = k_m = 10^2 \text{ M}^{-1} \text{ s}^{-1}$) is kinetically competent for the epoxidation of TME by NO as catalyzed by (Cl₈TPP)Fe^{III}Cl. The simulated percentage yields of products are provided in Table VII. These data compare most favorably to the experimentally determined percentage yields which have been shown in Table III.

It was an intention to employ 2,4,6-tri-*tert*-butylphenol (TBPH) as a trap for the iron(IV)-oxo porphyrin π -cation radical species generated on oxygen atom transfer from NO to (Cl₈TPP)Fe^{III}Cl. This hope was dashed on finding that not all high valent iron-oxo porphyrin species could be trapped at the highest concentration of TBPH that could reasonably be employed (Table I). When the reactions of Scheme II are amended by addition of eq n, o, p, and q, the appearance of TBP• with time (monitored at 630 nm) can be fitted. In order to do so, the rate constants of Table



IV, with the exception of k_b and k_f , were used. The values of k_n , k_o , k_p , and k_q were set equal to $5.2 \times 10^3 \text{ M}^{-1} \text{ s}^{-1}$ to provide the correct yields of the radical TBP• as well as DA and MA. When employing Scheme II plus eq n, o, p, and q with their associated constants to fit the experimental data of Figure 3, it is found that

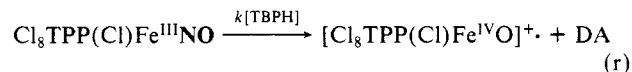
Table VIII. Percentage Yields of Products which Correspond to the Simulated Time Course (Figure 3) for Oxidation of 2,4,6-Tri-*tert*-butylphenol by NO ($=2.4 \times 10^{-3}$ M) in the Presence of (Cl₈TPP)Fe^{III}Cl ($=8.0 \times 10^{-5}$ M)

% yields			
[TBPH] _i , M	DA	MA	TBP•
0.03	58	42	37
0.06	62	38	48
0.15	74	26	67
0.30	83	17	79

it is necessary to assume that an increase in [TBPH]_i increases the rate constant for decomposition of the Cl₈TPP(Cl)Fe^{III}NO complex (k_b) and decreases the rate constant for decomposition of the Cl₈TPP(NO)Fe^{III}NO complex (k_f).

[TBPH] _i , M	k_b , s ⁻¹	k_f , s ⁻¹
0	5.0×10^{-2}	0.47
0.03	5.0×10^{-2}	0.47
0.06	4.0×10^{-2}	0.38
0.15	7.0×10^{-2}	0.35
0.30	7.5×10^{-2}	0.32

The fits of the experimental data points of Figure 3 can also be made by employing the constants of Table IV along with those for k_n , k_o , k_p , and k_q if it is assumed that TBPH is a catalyst for decomposition of the mono *N*-oxide complex (as in eq r).



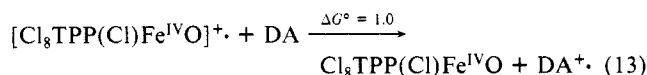
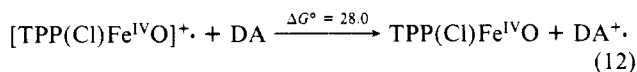
The values of k_b , k_f , and k_r employed to generate the lines of Figure 3 are

[TBPH] _i , M	k_b , s ⁻¹	k_f , s ⁻¹	k_r , M ⁻¹ s ⁻¹
0	5.0×10^{-2}	0.47	
0.03	5.0×10^{-2}	0.47	5.0×10^{-2}
0.06	4.0×10^{-2}	0.35	4.0×10^{-2}
0.15	5.0×10^{-2}	0.40	5.0×10^{-2}
0.30	5.0×10^{-2}	0.40	5.0×10^{-2}

By either means of fitting, TBPH provides a very modest increase in the rate of decomposition of the mono *N*-oxide complex as compared to the rate of decomposition of the bis *N*-oxide complex. These changes amount to only a few hundreded calories/mole in free energies of activation and may be considered as trivial. The reaction sequence of Scheme II, plus eq n, o, p, and q, is deemed competent to explain the oxidation of TBPH. The percentage yields generated by simulation are shown in Table VIII. Comparison of the predicted percentage yields to the experimentally determined yields of products (Table I) shows near identity.

When comparing the rates of reactions of [TPP(X)Fe^{IV}O]⁺ and [Cl₈TPP(X)Fe^{IV}O]⁺ with a given substrate, one must take into consideration that the latter should be a much better oxidant (as shown by electrochemical data, eq 7 and 8) but that approach to either the oxo ligand (for epoxidation or electron transfer) or to the porphyrin ring structure (for electron transfer) is sterically hindered by the eight chloro substituents. The lessened ability of TBPH to trap (by electron-transfer oxidation) the iron(IV) octachloroporphyrin π -cation species, when compared to the reaction when using (TPP)Fe^{III}Cl as the catalyst, may be attributed to this steric hindrance. Steric hindrance of the approach of TBPH to the iron(IV)-oxo octachlorotetraphenylporphyrin π -cation radicals must be greater than that for approach of DA. The oxidations of TBPH and DA are 1e⁻-transfer processes and thus differ from the epoxidation of alkenes. It is yet to be determined whether 1e⁻ oxidation or epoxidation is most affected by a decrease in the electron density of the porphyrin ligand brought about by substitution with electronegative substituents. That the rate constant for oxidation of DA should be greatly increased due to the electron withdrawal of the octachloro substituents can be appreciated by consideration of the differences in the standard free energies (kilojoule/mole) of oxidation of DA. From a knowledge of the potentials for the 1e⁻ reductions of [TPP(Cl)-

$\text{Fe}^{\text{IV}}\text{O}]^+$ and $[\text{Cl}_8\text{TPP}(\text{Cl})\text{Fe}^{\text{IV}}\text{O}]^+$ (eq 7 and 8) and the $1e^-$ reduction of DA^+ (1.45 V),^{1d} one can calculate the standard free energies for DA oxidation by the iron(IV)-oxo porphyrin π -cation radicals.



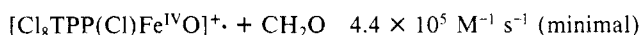
Allowable Comparisons of the Dynamics for the Reaction of *p*-Cyano-*N,N*-dimethylaniline *N*-Oxide with (TPP)Fe^{III}Cl and (Cl₈TPP)Fe^{III}Cl. Oxygen transfer from NO to (TPP)Fe^{III}Cl follows an endergonic complexation of reactants and is clearly rate-determining in the turnover of the catalyst. Oxygen transfer, under the concentrations employed (similar to the present study), involves only the mono *N*-oxide iron(III) porphyrin complex. The intermediate $[\text{TPP}(\text{Cl})\text{Fe}^{\text{IV}}\text{O}]^+$ species is trapable with either TBPH or TME. The formation of $[\text{TPP}(\text{Cl})\text{Fe}^{\text{IV}}\text{O}]^+$ follows the first-order rate law, and the computed second-order rate constant for the oxygen-transfer reaction is a product of the separately undeterminable constants for complexation of (TPP)Fe^{III}Cl by NO and the intracomplex oxygen transfer to yield $[\text{TPP}(\text{Cl})\text{Fe}^{\text{IV}}\text{O}]^+$ plus DA. On the other hand, oxygen transfer from NO to (Cl₈TPP)Fe^{III}Cl involves both a mono and a bis *N*-oxide complex with the iron(III) porphyrin. The formation of the mono complex is exergonic, and the catalyst is saturated with NO through much of the time course for the reaction. The equilibrium constant for formation of the monocomplex has been computed but that for bis complex formation is unavailable since this process is unfavorable at the concentrations of iron(III) porphyrin and NO employed. With these considerations in mind, it is obvious that the values of the equilibrium constants for NO complexation by (TPP)Fe^{III}Cl and (Cl₈TPP)Fe^{III}Cl cannot be compared nor can the rate constants for intracomplex oxygen transfer with $[\text{TPP}(\text{Cl})\text{Fe}^{\text{IV}}\text{O}]^+$ and $[\text{Cl}_8\text{TPP}(\text{Cl})\text{Fe}^{\text{IV}}\text{O}]^+$ or $[\text{Cl}_8\text{TPP}(\text{NO})\text{Fe}^{\text{IV}}\text{O}]^+$. Comparison of the products of the complexing constant (k_a/k_{-a}) and first-order rate constants for oxygen transfer (k_b) can be made:

	$(k_a/k_{-a}),$ M^{-1}	k_b, s^{-1}	$(k_a k_b/k_{-a}),$ $\text{M}^{-1} \text{s}^{-1}$
NO + (TPP)Fe ^{III} Cl			5–7
NO + (Cl ₈ TPP)Fe ^{III} Cl	1×10^4	4×10^{-2}	4×10^2

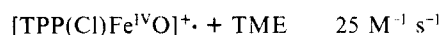
The overall rate constant ($k_a k_b/k_{-a}$) for oxygen transfer is increased 100-fold by the octachloro substitution.

The only products formed in the case of the decomposition of NO by (Cl₈TPP)Fe^{III}Cl are DA and MA. When (TPP)Fe^{III}Cl is employed as the catalyst, four additional products are also obtained: *N*-formyl-*p*-cyano-*N*-methylaniline (FA), *p*-cyanoaniline (A), *N,N*-bis(*p*-cyanophenyl)-*N*-methylmethylenediamine (MD), and *N,N'*-dimethyl-*N,N'*-bis(*p*-cyanophenyl)hydrazine (H). This result suggests that oxidations of DA and CH₂O by $[\text{Cl}_8\text{TPP}(\text{Cl})\text{Fe}^{\text{IV}}\text{O}]^+$ and $[\text{Cl}_8\text{TPP}(\text{NO})\text{Fe}^{\text{IV}}\text{O}]^+$ are so much more facile than their oxidation by $[\text{TPP}(\text{Cl})\text{Fe}^{\text{IV}}\text{O}]^+$ that no further oxidations of MA or CAI to yield the other four products are seen when (Cl₈TPP)Fe^{III}Cl is the catalyst. Comparison of the potentials for $[(\text{Cl}_8\text{TPP})\text{Fe}^{\text{IV}}\text{OMe}]^+$ and $[(\text{TPP})\text{Fe}^{\text{IV}}\text{OMe}]^+$ establishes the former to be a stronger $1e^-$ oxidant by 280 mV (eq 7 and 8). The rate constants for the cascade of oxidations carried out by $[\text{TPP}(\text{Cl})\text{Fe}^{\text{IV}}\text{O}]^+$ could be obtained by simulation even though these steps occur after the rate-limiting oxygen-transfer reaction. As in the present study, the ratios of the products dictate the ratios of the rate constants for product-forming steps. The maximum values of these rate constants were set by the observation of lag phases in product formation and the minimum values by the known constant for the rate-determining step. In the instance of the $[\text{Cl}_8\text{TPP}(\text{Cl})\text{Fe}^{\text{IV}}\text{O}]^+$ oxidations, there could only be set minimum values for the rate constants based on the fact that product formation was not accompanied by a lag period. A comparison of the rate constants for the oxidation of DA and CH₂O by $[\text{TPP}(\text{Cl})\text{Fe}^{\text{IV}}\text{O}]^+$ to the determined minimum values of these constants

for $[\text{Cl}_8\text{TPP}(\text{Cl})\text{Fe}^{\text{IV}}\text{O}]^+$ is informative:



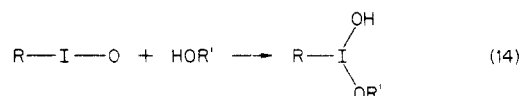
The octachloro-substituted iron(IV)-oxo tetraphenylporphyrin π -cation radical is minimally 1000-fold better an oxidant for DA oxidation and 300-fold better for CH₂O oxidation. Octachloro substitution of the iron(IV)-oxo porphyrin π -cation radical provides a minimal increase in the rate of TME epoxidation of 4-fold:



As with (TPP)Fe^{III}Cl catalysis, it was our hope that we might be able to assign second-order rate constants to the epoxidation of alkenes by (Cl₈TPP)Fe^{III}Cl. This has not been possible. Since k_1 and k_m are set relative to k_2 and k_j and the latter constants are minimal, the constants k_1 and k_m are also minimal. Thus, as long as k_c , k_g , k_j , and k_k are maintained at the proper ratios to provide the correct product ratios, they may be increased beyond their given minimum values until the largest constant becomes diffusion-limited without affecting the fits of the kinetic plots. The second-order rate constants for the epoxidation reactions cannot, therefore, be given as other than minimal values.

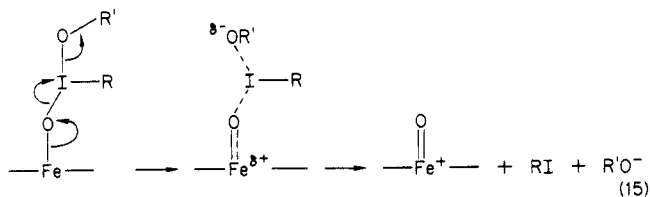
Finally, even though the ability of $[\text{Cl}_8\text{TPP}(\text{Cl})\text{Fe}^{\text{IV}}\text{O}]^+$ to epoxidize the alkenes in Table II is much greater than that of $[\text{TPP}(\text{Cl})\text{Fe}^{\text{IV}}\text{O}]^+$, higher yields of epoxidation are obtained when employing (TPP)Fe^{III}Cl as the catalyst. This result is due to the fact that the ratios of the rate constants for DA and CH₂O oxidation to the rate constants for TME oxidation are $3.4 \times 10^3/1$ and $4.4 \times 10^3/1$, respectively, when the catalyst is (Cl₈TPP)Fe^{III}Cl while when the catalyst is (TPP)Fe^{III}Cl, these ratios are 12/1 and 60/1, respectively. Thus, in comparing the oxidative selectivity of the iron(IV) porphyrin π -cation radicals generated from (Cl₈TPP)Fe^{III}Cl and (TPP)Fe^{III}Cl, one notices that the octachloro species is 300 times more selective toward DA oxidation as compared to TME epoxidation and about 70 times more selective toward CH₂O oxidation as compared to TME epoxidation. Employing reactions l and m for cyclohexene epoxidation, one can calculate relative rate constants for cyclohexene epoxidation by $[\text{Cl}_8\text{TPP}(\text{Cl})\text{Fe}^{\text{IV}}\text{O}]^+$ and $[\text{Cl}_8\text{TPP}(\text{NO})\text{Fe}^{\text{IV}}\text{O}]^+$. From these calculations, cyclohexene epoxidation is 1.6 times as fast as TME epoxidation. In the case of (TPP)Fe^{III}Cl, TME is epoxidized twice as fast as cyclohexene. *cis*- and *trans*-stilbene and norbornylene do not compete with DA as substrates for the iron(IV)-oxo octachlorotetraphenylporphyrin π -cation radical. This is not so with the iron(IV)-oxo tetraphenylporphyrin π -cation radical. These results establish the role of steric hindrance in the epoxidation of alkenes by the iron(IV) porphyrin π -cation radicals generated from (Cl₈TPP)Fe^{III}Cl.

By far and away the most effective porphyrin-based epoxidation system has been reported by Traylor and co-workers.¹⁰ Their system consists of (Cl₈TPP)Fe^{III}Cl and pentafluoriodosylbenzene in a solvent of CH₂Cl₂ containing 18% CH₃OH and 2% H₂O. The actual oxygen-transfer agent is proposed to arise via reaction of the alcohol with iodosylbenzene as shown in eq 14. Oxygen



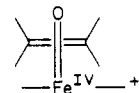
transfer is suggested to occur by way of the mechanism in eq 15. The oxo species of eq 15 is presumably identical with $[\text{Cl}_8\text{TPP}(\text{Cl})\text{Fe}^{\text{IV}}\text{O}]^+$ of this study. A rather amazing feature of the Traylor system is that there is no apparent steric effect in the

(10) Traylor, T. G.; Marsters, J. C., Jr.; Nakano, T.; Dunlap, B. E. *J. Am. Chem. Soc.*, in press.



epoxidation reaction. That we find that it is necessary to involve a steric effect when using NO as the oxygen transfer agent suggests that in the case of oxygen transfer from NO to $(\text{Cl}_8\text{TPP})\text{Fe}^{\text{III}}\text{Cl}$, subsequent DA oxidation has very little steric requirement, and for this reason, DA oxidation competes most successfully with bulky arenes for the $[\text{Cl}_8\text{TPP}(\text{Cl})\text{Fe}^{\text{IV}}\text{O}]^+$ species. In Traylor's experiments, the steric effect would be of little importance because the $[\text{Cl}_8\text{TPP}(\text{Cl})\text{Fe}^{\text{IV}}\text{O}]^+$ is generated in the absence of all oxidizable substrates except for added alkene. When using either NO or pentafluoriodosylbenzene, the rate-limiting step is oxygen transfer with substrate oxidation being much faster. In such a situation, the ratios of products formed are dependent upon the rate constants for the added substrate reacting with $[\text{Cl}_8\text{TPP}(\text{Cl})\text{Fe}^{\text{IV}}\text{O}]^+$. Examination of molecular models for (Cl_8TPP) -

$\text{Fe}^{\text{III}}\text{Cl}$ and the X-ray data for $((\text{MeO})_8\text{TPP})\text{H}_2^{11}$ in conjunction with what would appear to be the most reasonable transition-state geometry for epoxidation¹² suggests that steric hindrance should be encountered when employing $(\text{Cl}_8\text{TPP})\text{Fe}^{\text{III}}\text{Cl}$ as the catalyst.



Acknowledgment. This work has been supported by a grant from The National Institutes of Health. We thank Prof. Teddy Traylor for allowing us to read his manuscript prior to its publication.

Registry No. TBPH, 732-26-3; TME, 563-79-1; $\text{Cl}_8(\text{TPP})\text{Fe}^{\text{III}}\text{Cl}$, 91042-27-2; *p*-cyano-*N,N*-dimethylaniline *N*-oxide, 62820-00-2; cyclohexene, 110-83-8.

(11) Gold, K. W.; Hodgson, D. J.; Gold, A.; Savrin, J. E.; Toney, G. E. *J. Chem. Soc., Chem. Commun.* **1985**, 563.

(12) (a) Collman, J. P.; Brauman, J. I.; Meunier, B.; Raybuck, S. A.; Kodadek, T. *Proc. Natl. Acad. Sci. U.S.A.* **1984**, *81*, 3245. (b) Groves, J. T.; Nemo, T. E. *J. Am. Chem. Soc.* **1983**, *105*, 5786.

Influence of Nitrogen Base Ligation and Hydrogen Bonding on the Rate Constants for Oxygen Transfer from Percarboxylic Acids and Alkyl Hydroperoxides to (*meso*-Tetraphenylporphinato)manganese(III) Chloride

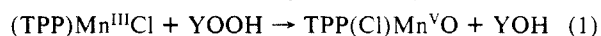
Lung-Chi Yuan and Thomas C. Bruice*

Contribution from the Department of Chemistry, University of California at Santa Barbara, Santa Barbara, California 93106. Received July 8, 1985

Abstract: Equilibrium constants for axial ligation of imidazole (ImH), *N*-methylimidazole (*N*-MeIm), 4'-(imidazo-1-yl)-acetophenone (NACPhIm), 2,6-lutidine (2,6-Py), and 3,4-lutidine (3,4-Py) with (*meso*-tetraphenylporphinato)manganese chloride $((\text{TPP})\text{Mn}^{\text{III}}\text{Cl})$ have been determined. The rates of oxygen atom transfer from percarboxylic acids and alkyl hydroperoxides (YOOH) to the manganese(III) porphyrin in the presence of varying concentrations of the nitrogen bases were determined. For this purpose, 2,2-diphenyl-1-picrylhydrazine (DPPH) was employed as a trap for the generated higher valent oxo-manganese porphyrin species. From the equilibrium and kinetic data, there was then calculated the second-order rate constants for oxygen atom transfer from YOOH compounds to the species $(\text{TPP})\text{Mn}^{\text{III}}\text{Cl}$, $\text{TPP}(\text{Cl})\text{Mn}^{\text{III}}\text{N}$, and $\text{TPP}(\text{Cl})\text{Mn}^{\text{III}}\text{N}_2$ (where N = ImH, *N*-MeIm, and 3,4-Py). Only the percarboxylic acids exhibit measurable rate constants for oxygen transfer to $(\text{TPP})\text{Mn}^{\text{III}}\text{Cl}$, whereas alkyl hydroperoxides and percarboxylic acids transfer oxygen to the $\text{TPP}(\text{Cl})\text{Mn}^{\text{III}}\text{N}$ species. Of the species $\text{TPP}(\text{Cl})\text{Mn}^{\text{III}}\text{N}_2$, reaction with YOOH compounds is seen only when N is imidazole. This is attributed to an equilibrium of the unreactive bis axially ligated $\text{TPP}(\text{Cl})\text{Mn}^{\text{III}}(\text{ImH})_2$ with the reactive isomeric mono axial-ligated complex $\text{Cl}^-\cdots\text{H}-\text{Im}\cdots\text{H}-\text{Im}\cdots\text{Mn}^{\text{III}}\text{TPP}$. Nitrogen base ligation of $(\text{TPP})\text{Mn}^{\text{III}}\text{Cl}$ provides minimally a 10^3 increase in the rate constants for oxygen transfer in methylene chloride. Linear free-energy plots of the log of the second-order rate constants for oxygen transfer from YOOH vs. the $\text{p}K_a$ of YOH establish that β_{ig} for oxygen transfer in which heterolytic O-O bond scission is rate-determining is large and negative. The value of β_{ig} when oxygen transfer involves rate-determining homolytic O-O bond scission is small and negative.

Sligar and co-workers have successfully demonstrated the reconstitution of P-450_{CAM} with manganese protoporphyrin IX with retention of enzyme activity.¹ Model studies of P-450 and peroxidase have been focused on the investigations with manganese porphyrins, as well as iron porphyrins. A puzzling observation which has received much attention is that though manganese(III) porphyrin salts are good catalysts for oxidations with iodosylbenzene and percarboxylic acids, they are not reactive with alkyl hydroperoxides.²⁻⁵ We have recently shown that the lack of

reactivity of $(\text{TPP})\text{Mn}^{\text{III}}\text{Cl}$ with alkylhydroperoxides in benzonitrile is due to the very great sensitivity of the oxygen transfer to the acidity of the leaving group (YOH), eq 1.⁵ On the other



hand, the reactivity and stereoselectivity of manganese(III)

(2) Hill, C. L.; Smegal, J. A.; Henly, T. J. *J. Org. Chem.* **1983**, *48*, 3277.
(3) Mansuy, D.; Bartoli, J.-F.; Momenteau, M. *Tetrahedron Lett.* **1982**, 23, 2781.

(4) Mansuy, D.; Bartoli, J.-F.; Chottard, J.-C.; Lange, M. *Angew. Chem., Int. Ed. Engl.* **1980**, *19*, 909.

(5) Yuan, L. C.; Bruice, T. C. *Inorg. Chem.* **1985**, *24*, 986.

(1) Gelb, M. H.; Toscano, W. A., Jr.; Sligar, S. G. *Proc. Natl. Acad. Sci. U.S.A.* **1982**, *79*, 5758.